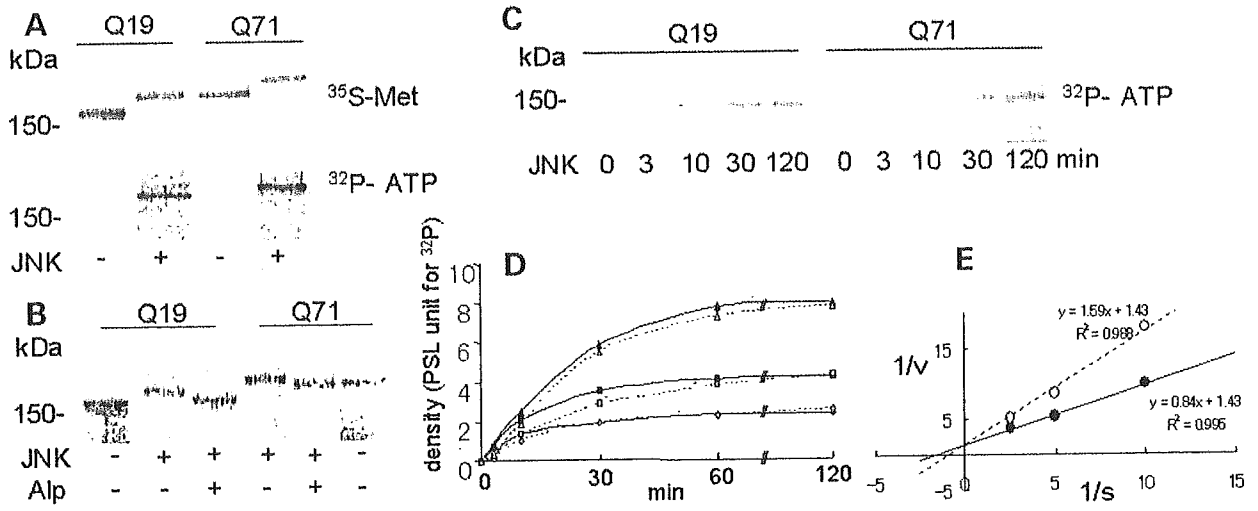

Figure 3. Phosphorylation of the full-length DRPLA protein in the recombinant activation system for JNK. In vitro translation products of the full-length DRPLA protein containing normal (Q19) and abnormal (Q71) polyQ were incubated in the recombinant JNK mixture. (A) The DRPLA protein labeled with [^{35}S]methionine (^{35}S-Met) was treated with or without the JNK reaction mixture (+ or −) for 1 h and applied on SDS–PAGE (upper panel). Non-labeled DRPLA protein was incubated in the mixtures containing [γ-^{32}P]ATP for 1 h and the phosphorylation was detected by autoradiography (lower panel). (B) The DRPLA protein labeled with [^{35}S]methionine was treated with or without alkaline phosphatase (Alp + or −), and resolved through SDS–PAGE with parallel run of products incubated in an incomplete JNK reaction mixture (JNK−). The indicated lanes were the results after omission of recombinant JNK, omission of any member of four kinases from the reaction abolished the mobility shift as well as incorporation of [γ-^{32}P]ATP. (C–E) Kinetic analysis of phosphorylation of the DRPLA protein by JNK. In vitro translation products (diamond, 1 U; square, 2 U; and triangle, 4 U) of the normal (Q19, solid symbols) and abnormal (Q71, open symbols) DRPLA proteins were incubated in 10 µl of the JNK mixture containing [γ-^{32}P]ATP for the indicated periods, and subjected to SDS–PAGE. A representative result of the autoradiographs in duplicates of three independent experiments is shown in (C). The extent of phosphorylation was quantified with radioactivity in the target proteins and plotted along incubation periods (D). The initial velocity (v) was calculated in the substrate content (s), and the double reciprocal plot (1/v versus 1/s) was used for evaluation of K_m (E).

kinetic analysis showed that the affinity of JNK for the abnormal protein was lower than that of the normal protein ($K_m = 0.59$ U/µl for the normal protein and 1.11 U/µl for the abnormal protein in Fig. 3E). Thus, the expanded polyQ reduced the affinity of JNK for the DRPLA protein.

To further investigate the phospho-acceptor sites, we produced seven non-overlapping fragments of the DRPLA protein (DR-a–i, shown in Fig. 1A). When subjected to the recombinant system, one of the fragments, DR-f, was strongly phosphorylated in the mixture (Fig. 4). In the absence of recombinant JNK3, the phosphorylation was completely eliminated (lanes f and f* in Fig. 4; note that the band for JNK3 also disappeared in lane f*). This clearly showed that the DR-f fragment was directly phosphorylated by JNK3. When the fragment was separated into two portions (DR-h and -i in Fig. 1A), both were phosphorylated (Fig. 4, lanes h and i). Thus, DR-f was thought to contain at least two phospho-acceptor sites, one of which was located in DR-h and the other in DR-i. Although the details were not examined, two other fragments, DR-a and -g, seem to have additional minor phospho-acceptor sites (Fig. 4, lanes a and g).

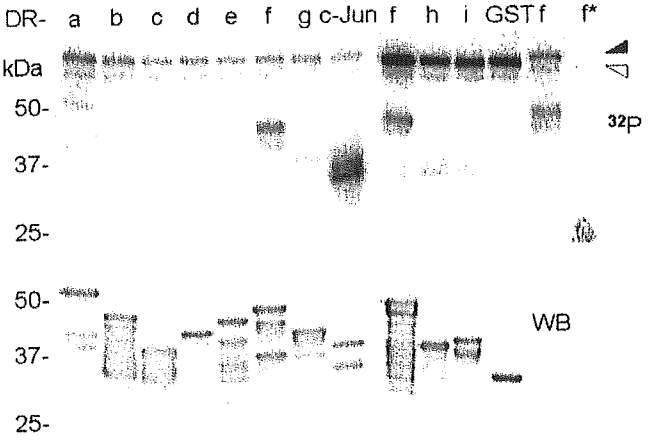

Figure 4. Phosphorylation of fragments of the DRPLA protein in the recombinant activation system for JNK. Equivalent amounts of the fragments of the DRPLA protein (DR-a–i, illustrated in Fig. 1A) were produced as GST-fusion proteins and visualized in western blotting with an anti-GST antibody (lower panels). They were incubated in the mixture containing JNK3 (closed triangle in upper panels), MKK4 (open triangle), constitutive active forms of MKK7 and MEKK1, and [γ-^{32}P]ATP for 30 min. The phosphorylation is detected with the radioactivity of the fragments (upper panels). Recombinant JNK3 was omitted in the last lane (f*). GST and c-Jun were used as positive and negative control substrates. Experiments were repeated three times and representative results are shown.

DRPLA protein over-expressed in cells was phosphorylated by JNK

Endogenous DRPLA protein was phosphorylated as shown in Figure 2. Then, we tested the phosphorylated state of over expressed forms of the normal and abnormal protein, tagged with HA at the N-terminal end, in neuroblastoma cells (Fig. 5). We chose a high osmotic pressure by adding sorbitol to the cultured medium for transient activation of JNK. As demonstrated in Figure 5A, active JNK was increased to

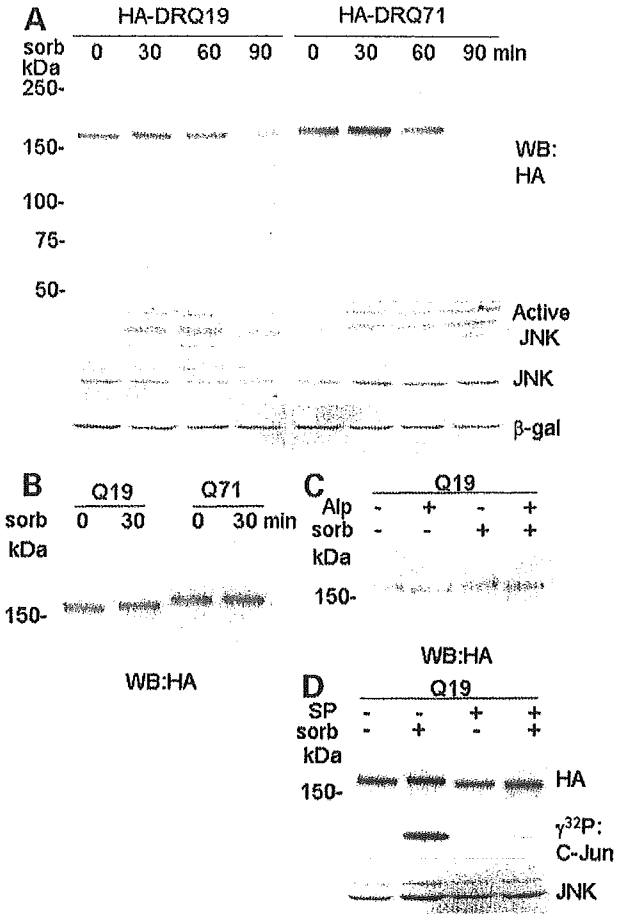

Figure 5. The overexpressed DRPLA protein is phosphorylated by JNK. Cells expressing HA-tagged normal and abnormal forms of the DRPLA protein (HA-DRQ19 and Q71) were incubated under a high osmotic condition with sorbitol for the indicated period (otherwise 30 min). The over-expressed protein was detected by western blotting with an anti-HA antibody (HA). The cell lysates were treated with alkaline phosphatase (Alp + in the panel C). The cells were incubated with the addition of JNK inhibitor, SP600125 (SP + in the panel D). The activity of JNK was monitored by western blotting with anti-active JNK antibody and by immune-complex kinase assay with c-Jun (A and D). The amount of total JNK and an unrelated protein (acid β-galactosidase) were monitored by western blotting with anti-JNK and β-galactosidase antibodies (D).

be detectable by western blotting with an anti-active JNK antibody. Along with the stimulation, amounts of the overexpressed forms of the DRPLA protein decreased afterward. It seemed that the N-terminal portion was cleaved off in the process, although the smaller fragments were not detected with the anti-HA antibody.

We examined the mobility shift of the normal DRPLA protein expressed in cells after osmotic stress. The mobility shift of the normal DRPLA was clear after 30 min of the stimulation (Fig. 5B), although the extent of the mobility shift shown here was less than that shown in the recombinant system (Q19 in Fig. 3A). The mobility shift of the abnormal protein was imperceptible. After the treatment of cell lysates with alkaline phosphatase, the normal protein with the osmotic stress migrated to the basal position without stress (Fig. 5C). Thus, the mobility shift was due to the phosphorylation state. When the cells were treated with a selective inhibitor of JNK, SP600125 (41) in the osmotic stress condition, the JNK kinase activity was inhibited as expected, and the normal protein migrated to the same position as the cells without osmotic stress (Fig. 5D). These results showed that DRPLA protein overexpressed in cultured cells was phosphorylated by JNK.

Serine 734 of the DRPLA protein is a phospho-acceptor site by JNK

We focused on phosphorylation of serine 734 (S734) in the DR-i fragment of DRPLA protein (double-underlined in Fig. 1B), because the flanking sequence, PESP, exactly matched the consensus sequence of phosphorylation by MAPKs (33). Moreover, the following sequence to S734 (SPVPP) is also found in BCL-2 (Fig. 1B) and the serine residue in the BCL-2 sequence is phosphorylated by JNK (42). To determine if the S734 residue in the DRPLA protein is essential for phosphorylation with JNK, we constructed a mutant fragment, DR-i734A, in which S734 was substituted to alanine. In contrast to the normal counterpart, the mutant fragment was not phosphorylated in the recombinant activation system and the immune complex kinase assay for JNK (Fig. 6A and B).

To show immunological evidence for phosphorylation of S734, we produced two antibodies (epitopes of which are shown in Fig. 1B) and assessed their specific reactivity in ELISA assay (Fig. 6C). The raised anti-phosphoserine 734 antibody (anti-DRs) reacted with the phosphorylated DR-i fragment in the recombinant JNK system, but not with non-phosphorylated counterparts in western blotting. The anti-DRPLA peptide antibody (anti-DRb) reacted with both (Fig. 6D). These results were consistent with the recombinant JNK system described above, and the S734 residue was the main target by JNK.

Serine 734 is phosphorylated in the rat brain

The rat DRPLA protein has 93% homology to its human counterpart and is smaller by two amino acid residues (43). Since the peptide sequences used for raising the anti-phosphopeptide antibodies are exactly the same in both species (Fig. 1B), we analyzed the phosphorylated state of the rat DRPLA protein by western blotting with the raised antibodies (Fig. 7). The expression level of the DRPLA protein detected with the anti-DRb antibody was consistent with our previous results on the level of mRNA in northern blotting (4); where it was high in the brain and low in the pancreas and testis (Fig. 7A). The major form in the brain (150 kDa protein) was also reactive with the anti-DRs antibody, which indicated that S734 in the DRPLA protein in the rat brain tissues was phosphorylated (Fig. 7B). This form was also detected with the anti-DRa antibody (data not shown). When the brain samples were treated with alkaline phosphatase, the major form migrated faster and almost lost the immunoreactivity to the anti-DRs antibody (Fig. 7C). These data were consistent with phosphorylation at S734.

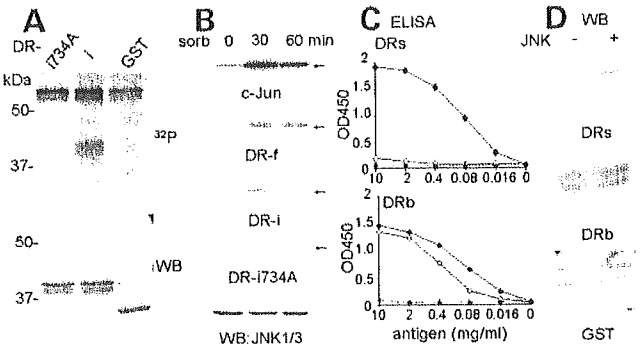

Figure 6. Serine 734 in the DRPLA protein is phosphorylated by JNK in vitro. (A) The fragment of DRPLA protein (DR-i), and its mutant form (DR-i734A, in which serine 734 was substituted to alanine) were subjected to the phosphorylation study with the recombinant activation system for JNK. (B) The indicated fragments of the DRPLA protein and c-Jun (with arrows) were used as a substrate for the immune-complex kinase assay of JNK. The neuroblastoma cells were treated with sorbitol for the indicated periods. Immunoprecipitated JNK was incubated with substrates and [γ-^{32}P]ATP. The phosphorylation of substrates was visualized by autoradiography. The amounts of precipitated JNK were monitored by western blotting (the last panel). (C) Specificity of two anti-peptide antibodies was tested by ELISA. Synthesized phosphorylated peptides (solid symbols), used for generating antibodies (DRs and DRb), and the non-phosphorylated counterparts (open symbols) were the antigen. Solid lines are for antibodies, and dotted lines for non-immune sera. (D) Anti-DRs antibody reacts with the fragment of DRPLA protein after phosphorylation by JNK. The fragment DR-i, treated with or without the recombinant JNK (+ or −), was blotted with anti-DRs, DRb and GST antibodies.

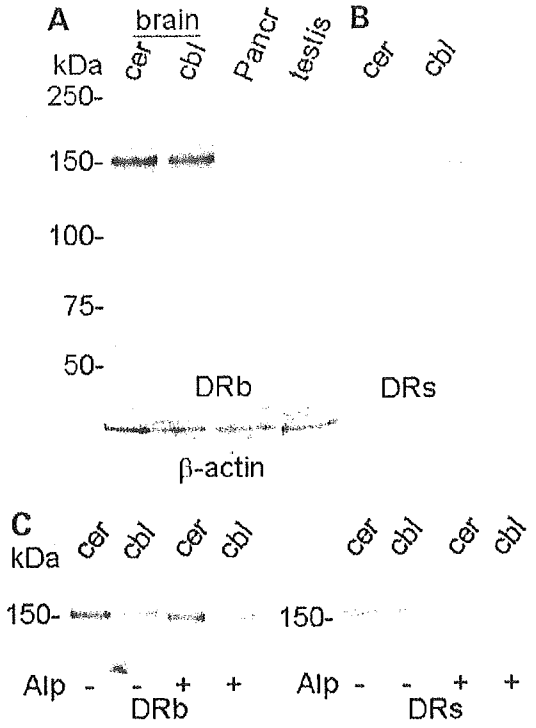

Figure 7. Serine 734 in the DRPLA protein in rat tissues is phosphorylated. (A–C) Western blotting of the DRPLA protein in rat tissues. Samples (30 μg of protein) obtained from the cerebrum (cer), cerebellum (cbl), pancreas (pancr) and testis were blotted with the anti-DRb, anti-DRs and anti-β actin antibodies. The brain samples in the parallel run were blotted with the anti-DRs in B. Samples were treated with or without alkaline phosphatase (Alp + or −) in (C).

DISCUSSION

We report evidence for phosphorylation of the DRPLA protein, the product of the gene responsible for the polyglutamine disease, dentatorubral-pallidoluysian atrophy. The endogenous form was phosphorylated and the phosphorylation was mainly mediated by JNK.

JNK is activated in the critical process of embryonic morphogenesis, as well as in response to environmental stress such as radiation and high osmotic pressure (44). The activation of JNK requires its phosphorylation mediated by MKK 4 and 7 (38,39). These two MKKs are activated by MKK kinases such as MEKK1. Activated JNK phosphorylates subsets of proteins including c-Jun, and up-regulates transcriptions of stress-responsive genes in various cells (45,46). In neurons, JNK3 is highly and consistently phosphorylated because of the synergistic activation of MKK4 and 7. Thus, DRPLA, one of the substrates of JNK3 as demonstrated in this report, may have a function in the brain coupled with activated JNK (47–49).

We identified the S734 residue of the DRPLA protein as a phospho-acceptor site in the recombinant system as well as in the brain tissues. However, phosphorylation of this residue was not detectable with the endogenous form of DRPLA protein in cultured cells with the same technique (data not shown). This may be accounted for by a weaker activity of JNK in cultured cells, while consistent activation of JNK is known in the brain at a similar level of the recombinant JNK system (49). The phosphorylation may be coupled to the activation of a protease. The molecular size of DRPLA protein detected in the rat brain with the specific phosphopeptide antibody was 150 kDa, which was slightly smaller than that expected from the sequence and the results with the human protein. The phosphorylated forms of HA-tagged human DRPLA gradually disappeared after osmotic treatment, as demonstrated in Fig. 5. Although we did not directly detect degraded forms, caspase-3 may be one of the candidates involved. We previously reported the DRPLA protein is a substrate of caspase-3 and about 10 kDa from the N-terminus was cleaved off (24).

Both the normal and abnormal forms of DRPLA protein were phosphorylated by the JNK recombinant system. However, precise kinetic analyses showed a reduced affinity of JNK for the abnormal protein. Furthermore, the abnormal protein expressed in cultured cells showed a subtle mobility shift in the JNK activation condition with osmotic pressure. It may be possible that a slight reduction of the affinity in the in vitro system causes considerable effects in a physiological condition, i.e. delay in a certain cascade reaction. Two other polyglutamine disease products, Huntingtin and androgen receptor, have recently been reported to be phosphorylated by an S/T kinase, Akt, which mediates the survival signal of IGF-I (50–52). As the DRPLA protein is already known to be situated in the insulin/IGF-I signaling cascade (25), three polyglutamine diseases products seem to be connected by the signal transduction of IGF-I. As IGF-I is one of the main neurotrophic factors, neurodegeneration in polyglutamine diseases may be solved by a function of IGF-I.

MATERIALS AND METHODS

Plasmid constructions

Original cDNA clones for DRPLA were previously described (2,4). The DNA fragment including the entire coding region of the DRPLA gene was subcloned into pBluescript SK(−) phagemid (Stratagene) for in vitro translation experiments, and a cpDNA-3xHA vector (kindly provided by Dr John C. Reed) for expression of HA-tagged proteins. cDNA fragments (shown in Fig. 1A) amplified by PCR methods were subcloned into a pGEX-3X vector (Pharmacia) to generate GST fusion proteins. Plasmid harboring a point mutation was obtained by PCR-mediated mutagenesis (53).

Antibodies

Epitopes for the following three antibodies are indicated in Figure 1. A rabbit polyclonal antibody which specifically reacted to a phosphorylated serine 734 residue in the DRPLA protein (anti-DRs) was raised against phosphopeptide ETPEpSPVPP (MBL Nagoya Japan). The serum was affinity-purified with the antigen peptide, and the reactivity to the non-phosphorylated peptide was eliminated with the affinity column. An anti-DRPLA peptide antibody (anti-DRb) was raised against phosphopeptide RSPpSPPPK, but it unexpectedly reacted to the non-phosphorylated counterpart as well as the antigen peptide. A rabbit polyclonal antibody raised against the recombinant human DRPLA protein (anti-DRa) was described previously (24). The following antibodies are also used: polyclonal anti-JNK1 antibody C-17 (Santa Cruz), monoclonal anti-JNK antibody (Pharmingen), anti-activated JNK antibody (Promega), monoclonal anti-phosphoserine antibody PSR-45 (Sigma), anti-HA antibody (Roche), anti-β actin antibody (Santa Crutz) and anti-human acid β-galactosidase antibody (54).

Preparation of recombinant proteins

Fragments of the DRPLA protein fused with GST were produced and purified as described previously (25). Translation products of the full-length DRPLA genes were produced with the TNT coupled reticulocyte lysate mixture in vitro (Promega). The radio-labeled and non-labeled products were made in the presence and absence of [^{35}S]methionine, respectively. To quantify the translation products, the labeled mixture was resolved by SDS–PAGE, and the radioactivity of the DRPLA protein was measured as Photo-Stimulated Luminescence (PSL) with a Fuji BAS 2000 PhosphorImager (Fuji Film, Japan). One unit (U) was defined as an amount of the mixture which gave 1 PSL unit/min of ^{35}S. The non-labeled mixtures, equivalent to 1, 2 and 4 U of the labeled counterparts, were subjected to the in vitro phosphorylation study.

In vitro phosphorylation assay in a recombinant activation system for JNK

In the recombinant system, JNK3 was synergistically activated by two forms of MKK, constitutive active MKK7 and native MKK4 that is activated by constitutive active MEKK1, as described previously (38–40). The mixture contains 100 ng of four GST-fusion proteins, JNK3, MKK4, MKK7 and MEKK1, in kinase buffer (50 mM Tris–Cl pH 7.5, 10 mM $MgCl_2$, 125 μM ATP, 1 mM DTT, 2 mM EDTA-Na and 500 μM $NaVO_4$). The fragments of the DRPLA protein fused with GST (100 ng equivalent) and the in vitro translation products of the DRPLA protein (1–4 U) were incubated in 10 μl of the mixture, with 5 μCi of [γ-^{32}P]ATP if needed, at 30°C for the indicated periods. Samples were resolved by SDS–PAGE and visualized with the PhosphorImager.

Cell culture

A human neuroblastoma cell line, SH-SY5Y, was maintained in RPMI1640 with 10% fetal bovine serum and transfected with plasmids using Lipofectamine PLUS (GIBCOBRL). For the activation of JNK with high osmotic pressure, cells were pre-incubated in the medium with 500 μM of Na_3VO_4 for 15 min. Then D(−)-sorbitol was added at a final concentration of 1 M and the incubation was continued for the indicated periods. For inhibition of the JNK kinase activity, a reversible ATP-competitive inhibitor, SP600125 (25 μM, BIOMOL), was added to the media 15 min prior to the sorbitol stimulation (41).

Immune complex protein kinase assay

SH-SY5Y cells were lysed in a lysis buffer (20 mM Tris–Cl pH 7.5, 150 mM NaCl, 1 mM EDTA, 1 mM EGTA, 1% Triton X-100, 2.5 mM sodium pyrophosphate, 1 mM β-glycerolphosphate, 1 mM Na_3VO_4, 1 μg/ml leupeptin and 1 mM PMSF). The lysates were sonicated and centrifuged. An aliquot of cleared lysates (100 μg of protein) was immunoprecipitated with the anti-JNK antibody C-17 for 2 h. The immune complex was used for a kinase assay with 5 μCi of [γ-^{32}P]ATP and 2 μg of the GST-fusion protein in a kinase buffer (20 mM Hepes pH 7.4, 10 mM $MgCl_2$ and 200 μM Na_3VO_4). After incubation at 30°C for 30 min, the samples were resolved by SDS–PAGE. One-tenth of the immune complex was analyzed by western blotting with an anti-monoclonal anti-JNK antibody.

Phosphatase treatment

SH-SY5Y cells and tissues from adult rats (male, Wistar rats) were homogenized in the Tris/$MgCl_2$ buffer (50 mM Tris-Cl pH 7.5 and 1 mM $MgCl_2$), sonicated for 30 s and centrifuged. Cleared lysates were incubated with calf intestine alkaline phosphatase (2 U for 10 μg protein, Sigma) at 30°C for 15 min, and the reaction was terminated with phosphatase inhibitors (Sigma).

Western blotting, immunoprecipitation and ELISA assay

The details of procedures for immunoprecipitation and western blotting were described previously (25). Briefly, an aliquot containing 100 ng of GST-fusion proteins, and 30 μg of protein extracts was subjected to western blotting with 1:500, 1:500, 1:200, 1:200 and 1:1000 diluted anti-GST, DRa, DRb, DRs and HA antibodies, respectively. To confirm equal loading of protein samples, the blotted membranes were re-probed with

the 1:400 and 1:250 diluted anti-β actin and anti-β galactosidase antibodies, respectively. The endogenous DRPLA protein was immunoprecipitated with the anti-DRa antibody from 500 μg protein of cell lysates and blotted with the 1:100 diluted anti-phosphoserine antibody. The ELISA assay using synthetic peptides as antigens and titration assays with anti-DRb and anti-DRs antibodies were performed according to the standard methods.

ACKNOWLEDGEMENTS

We wish to acknowledge Professor Yoshiyuki Suzuki (International University of Health and Welfare) for important suggestions and critical reading of the manuscript. We also thank A. Asaka and Y. Ohtsuka for technical assistance and K. Saito for preparing the manuscript. This study was supported in part by Grants for Human Genome, Brain Science and Pediatric Research from the Ministry of Health, Labor and Welfare, and a Grant for Organized Research Combination System from the Ministry of Education, Culture, Sports, Science and Technology, Japan.

REFERENCES

1. Naito, H. and Oyanagi, S. (1982) Familial myoclonus epilepsy and choreoathetosis: hereditary dentatorubral-pallidoluysian atrophy. Neurology, 32, 798–807.
2. Nagafuchi, S., Yanagisawa, H., Sato, K., Shirayama, T., Ohsaki, E., Bundo, M., Takeda, T., Tadokoro, K., Kondo, I., Murayama, N. et al. (1994) Dentatorubral and pallidoluysian atrophy expansion of an unstable CAG trinucleotide on chromosome 12p. Nat. Genet., 6, 14–18.
3. Koide, R., Ikeuchi, T., Onodera, O., Tanaka, H., Igarashi, S., Endo, K., Takahashi, H., Kondo, R., Ishikawa, A., Hayashi, T. et al. (1994) Unstable expansion of CAG repeat in hereditary dentatorubral-pallidoluysian atrophy (DRPLA). Nat. Genet., 6, 9–13.
4. Nagafuchi, S., Yanagisawa, H., Ohsaki, E., Shirayama, T., Tadokoro, K., Inoue, T. and Yamada, M. (1994) Structure and expression of the gene responsible for the triplet repeat disorder, dentatorubral and pallidoluysian atrophy (DRPLA). Nat. Genet., 8, 177–182.
5. Zoghbi, H.Y. and Orr, H.T. (2000) Glutamine repeats and neurodegeneration. A. Rev. Neurosci., 23, 217–247.
6. Ikeda, H., Yamaguchi, M., Sugai, S., Aze, Y., Narumiya, S. and Kakizuka, A. (1996) Expanded polyglutamine in the Machado-Joseph disease protein induces cell death in vitro and in vivo. Nat. Genet., 13, 196–202.
7. Warrick, J.M., Paulson, H.L., Gray-Board, G.L., Bui, Q.T., Fischbeck, K.H., Pittman, R.N. and Bonini, N.M. (1998) Expanded polyglutamine protein forms nuclear inclusions and causes neural degeneration in Drosophila. Cell, 93, 939–949.
8. Orr, H.T. (2001) Beyond the Qs in the polyglutamine diseases. Genes Dev., 15, 925–932.
9. Monoi, H. (1995) New tubular single-stranded helix of poly-L-amino acids suggested by molecular mechanics calculations: I. Homopolypeptides in isolated environments. Biophys. J., 69, 1130–1141.
10. Miyashita, T., Nagao, K., Ohmi, K., Yanagisawa, H., Okamura-Oho, Y. and Yamada, M. (1998) Intracellular aggregate formation of dentatorubral-pallidoluysian atrophy (DRPLA) protein with the extended polyglutamine. Biochem. Biophys. Res. Commun., 249, 96–102.
11. Shimohata, T., Nakajima, T., Yamada, M., Uchida, C., Onodera, O., Naruse, S., Kimura, T., Koide, R., Nozaki, K., Sano, Y. et al. (2000) Expanded polyglutamine stretches interact with TAFII130, interfering with CREB-dependent transcription. Nat. Genet., 26, 29–36.
12. McCampbell, A., Taylor, J.P., Taye, A.A., Robitschek, J., Li, M., Walcott, J., Merry, D., Chai, Y., Paulson, H., Sobue, G. et al. (2000) CREB-binding protein sequestration by expanded polyglutamine. Hum. Mol. Genet., 9, 2197–2202.
13. Nucifora, F.C.J., Sasaki, M., Peters, M.F., Huang, H., Cooper, J.K., Yamada, M., Takahashi, H., Tsuji, S., Troncoso, J., Dawson, V.L. et al. (2001) Interference by huntingtin and atrophin-1 with cbp-mediated transcription leading to cellular toxicity. Science, 291, 2423–2428.
14. Bence, N.F., Sampat, R.M. and Kopito, R.R. (2001) Impairment of the ubiquitin-proteasome system by protein aggregation. Science, 292, 1552–1555.
15. Suhr, S.T., Senut, M.C., Whitelegge, J.P., Faull, K.F., Cuizon, D.B. and Gage, F.H. (2001) Identities of sequestered proteins in aggregates from cells with induced polyglutamine expression. J. Cell Biol., 153, 283–294.
16. Abel, A., Walcott, J., Woods, J., Duda, J. and Merry, D.E. (2001) Expression of expanded repeat androgen receptor produces neurologic disease in transgenic mice. Hum. Mol. Genet., 10, 107–116.
17. Cummings, C.J., Sun, Y., Opal, P., Antalffy, B., Mestril, R., Orr, H.T., Dillmann, W.H. and Zoghbi, H.Y. (2001) Over-expression of inducible HSP70 chaperone suppresses neuropathology and improves motor function in SCA1 mice. Hum. Mol. Genet., 10, 1511–1518.
18. Dorsman, J.C., Pepers, B., Langenberg, D., Kerkdijk, H., Ijszenga, M., den Dunnen, J.T., Roos, R.A. and van Ommen, G.J. (2002) Strong aggregation and increased toxicity of polyleucine over polyglutamine stretches in mammalian cells. Hum. Mol. Genet., 11, 1487–1496.
19. Ravikumar, B., Duden, R. and Rubinsztein, D.C. (2002) Aggregate-prone proteins with polyglutamine and polyalanine expansions are degraded by autophagy. Hum. Mol. Genet., 11, 1107–1117.
20. Jiang, H., Nucifora, F.C. Jr, Ross, C.A. and DeFranco, D.B. (2003) Cell death triggered by polyglutamine-expanded huntingtin in a neuronal cell line is associated with degradation of CREB-binding protein. Hum. Mol. Genet., 12, 1–12.
21. Klement, I.A., Skinner, P.J., Kaytor, M.D., Yi, H., Hersch, S.M., Clark, H.B., Zoghbi, H.Y. and Orr, H.T. (1998) Ataxin-1 nuclear localization and aggregation: role in polyglutamine-induced disease in SCA1 transgenic mice. Cell, 95, 41–53.
22. Saudou, F., Finkbeiner, S., Devys, D. and Greenberg, M.E. (1998) Huntingtin acts in the nucleus to induce apoptosis but death does not correlate with the formation of intranuclear inclusions. Cell, 95, 55–66.
23. Yu, Z.X., Li, S.H., Nguyen, H.P. and Li, X.J. (2002) Huntingtin inclusions do not deplete polyglutamine-containing transcription factors in HD mice. Hum. Mol. Genet., 11, 905–914.
24. Miyashita, T., Okamura-Oho, Y., Mito, Y., Nagafuchi, S. and Yamada, M. (1997) Dentatorubral pallidoluysian atrophy (DRPLA) protein is cleaved by caspase-3 during apoptosis. J. Biol. Chem., 272, 29238–29242.
25. Okamura-Oho, Y., Miyashita, T., Ohmi, K. and Yamada, M. (1999) Dentatorubral-pallidoluysian atrophy protein interacts through a proline-rich region near polyglutamine with the SH3 domain of an insulin receptor tyrosine kinase substrate. Hum. Mol. Genet., 8, 947–957.
26. Yanagisawa, H., Bundo, M., Miyashita, T., Okamura-Oho, Y., Tadokoro, K., Tokunaga, K. and Yamada, M. (2000) Protein binding of a DRPLA family through arginine-glutamic acid dipeptide repeats is enhanced by extended polyglutamine. Hum. Mol. Genet., 9, 1433–1442.
27. Okamura-Oho, Y., Miyashita, T. and Yamada, M. (2001) Distinctive tissue distribution and phosphorylation of IRSp53 isoforms. Biochem. Biophys. Res. Commun., 289, 957–960.
28. Coso, O.A., Chiariello, M., Yu, J.C., Teramoto, H., Crespo, P., Xu, N., Miki, T. and Gutkind, J.S. (1995) The small GTP-binding proteins Rac1 and Cdc42 regulate the activity of the JNK/SAPK signaling pathway. Cell, 81, 1137–1146.
29. Minden, A., Lin, A., Claret, F.X., Abo, A. and Karin, M. (1995) Selective activation of the JNK signaling cascade and c-Jun transcriptional activity by the small GTPases Rac and Cdc42Hs. Cell, 81, 1147–1157.
30. Miki, H., Yamaguchi, H., Suetsugu, S. and Takenawa, T. (2000) IRSp53 is an essential intermediate between Rac and WAVE in the regulation of membrane ruffling. Nature, 408, 732–735.
31. Axelrod, J.D., Miller, J.R., Shulman, J.M., Moon, R.T. and Perrimon, N. (1998) Differential recruitment of Dishevelled provides signaling specificity in the planar cell polarity and Wingless signaling pathways. Genes Dev., 12, 2610–2622.
32. Boutros, M., Paricio, N., Strutt, D.I. and Mlodzik, M. (1998) Dishevelled activates JNK and discriminates between JNK pathways in planar polarity and wingless signaling. Cell, 94, 109–118.
33. Clark-Lewis, I., Sanghera, J.S. and Pelech, S.L. (1991) Definition of a consensus sequence for peptide substrate recognition by p44mpk, the meiosis-activated myelin basic protein kinase. J. Biol. Chem., 266, 15180–15184.

34. Deng, T. and Karin, M. (1994) c-Fos transcriptional activity stimulated by H-Ras-activated protein kinase distinct from JNK and ERK. Nature, 371, 171–175.
35. Wood, J.D., Yuan, J., Margolis, R.L., Colomer, V., Duan, K., Kushi, J., Kaminsky, Z., Kleiderlein, J.J., Sharp, A.H. and Ross, C.A. (1998) Atrophin-1, the DRPLA gene product, interacts with two families of WW domain-containing proteins. Mol. Cell Neurosci., 11, 149–160.
36. Zhang, S., Xu, L., Lee, J. and Xu, T. (2002) Drosophila atrophin homolog functions as a transcriptional corepressor in multiple developmental processes. Cell, 108, 45–56.
37. Erkner, A., Roure, A., Charroux, B., Delaage, M., Holway, N., Core, N., Vola, C., Angelats, C., Pages, F., Fasano, L. et al. (2002) Grunge, related to human Atrophin-like proteins, has multiple functions in Drosophila development. Development, 129, 1119–1129.
38. Lawler, S., Fleming, Y., Goedert, M. and Cohen, P. (1998) Synergistic activation of SAPK1/JNK1 by two MAP kinase kinases in vitro. Curr. Biol., 8, 1387–1390.
39. Wada, T., Nakagawa, K., Watanabe, T., Nishitai, G., Kishimoto, H., Kitagawa, D., Sasaki, T., Penninger, J.M., Nishina, H. and Katada, T. (2001) Impaired synergistic activation of stress-activated protein kinase SAPK/JNK in mouse embryonic stem cells lacking SEK1/MKK4: different contribution of SEK2/MKK7 isoforms to the synergistic activation. J. Biol. Chem., 276, 30892–30897.
40. Sasaki, T., Wada, T., Kishimoto, H., Irie-Sasaki, J., Matsumoto, G., Goto, T., Yao, Z., Wakeham, A., Mak, T.W., Suzuki, A. et al. (2001) The stress kinase mitogen-activated protein kinase kinase (MKK)7 is a negative regulator of antigen receptor and growth factor receptor-induced proliferation in hematopoietic cells. J. Exp. Med., 194, 757–768.
41. Bennett, B.L., Sasaki, D.T., Murray, B.W., O'Leary, E.C., Sakata, S.T., Xu, W., Leisten, J.C., Motiwala, A., Pierce, S., Satoh, Y. et al. (2001) SP600125, an anthrapyrazolone inhibitor of Jun N-terminal kinase. Proc. Natl Acad. Sci. USA, 98, 13681–13686.
42. Yamamoto, K., Ichijo, H. and Korsmeyer, S.J. (1999) BCL-2 is phosphorylated and inactivated by an ASK1/Jun N-terminal protein kinase pathway normally activated at G(2)/M. Mol. Cell. Biol., 19, 8469–8478.
43. Loev, S.J., Margolis, R.L., Young, W.S., Li, S.H., Schilling, G., Ashworth, R.G. and Ross, C.A. (1995) Cloning and expression of the rat atrophin-I (DRPLA disease gene) homologue. Neurobiol. Dis., 2, 129–138.
44. Davis, R.J. (2000) Signal transduction by the JNK group of MAP kinases. Cell, 103, 239–252.
45. Pulverer, B.J., Kyriakis, J.M., Avruch, J., Nikolakaki, E. and Woodgett, J.R. (1991) Phosphorylation of c-jun mediated by MAP kinases. Nature, 353, 670–674.
46. Kyriakis, J.M., Banerjee, P., Nikolakaki, E., Dai, T., Rubie, E.A., Ahmad, M.F., Avruch, J. and Woodgett, J.R. (1994) The stress-activated protein kinase subfamily of c-Jun kinases. Nature, 369, 156–160.
47. Mohit, A.A., Martin, J.H. and Miller, C.A. (1995) p493F12 kinase: a novel MAP kinase expressed in a subset of neurons in the human nervous system. Neuron, 14, 67–78.
48. Yao, R., Yoshihara, M. and Osada, H. (1997) Specific activation of a c-Jun NH_2-terminal kinase isoform and induction of neurite outgrowth in PC-12 cells by staurosporine. J. Biol. Chem., 272, 18261–18266.
49. Coffey, E.T., Hongisto, V., Dickens, M., Davis, R.J. and Courtney, M.J. (2000) Dual roles for c-Jun N-terminal kinase in developmental and stress responses in cerebellar granule neurons. J. Neurosci., 20, 7602–7613.
50. Lin, H.K., Yeh, S., Kang, H.Y. and Chang, C. (2001) Akt suppresses androgen-induced apoptosis by phosphorylating and inhibiting androgen receptor. Proc. Natl Acad. Sci. USA, 98, 7200–7205.
51. Humbert, S., Bryson, E.A., Cordelieres, F.P., Connors, N.C., Datta, S.R., Finkbeiner, S., Greenberg, M.E. and Saudou, F. (2002) The IGF-1/Akt pathway is neuroprotective in Huntington's disease and involves Huntingtin phosphorylation by Akt. Dev. Cell, 2, 831–837.
52. Brunet, A., Datta, S.R. and Greenberg, M.E. (2001) Transcription-dependent and -independent control of neuronal survival by the PI3K-Akt signaling pathway. Curr. Opin. Neurobiol., 11, 297–305.
53. Imai, Y., Matsushima, Y., Sugimura, T. and Terada, M. (1991) A simple and rapid method for generating a deletion by PCR. Nucl. Acids Res., 19, 2785.
54. Okamura-Oho, Y., Zhang, S., Hilson, W., Hinek, A. and Callahan, J.W. (1996) Early proteolytic cleavage with loss of a C-terminal fragment underlies altered processing of the beta-galactosidase precursor in galactosialidosis. Biochem. J., 313, 787–794.

American Journal of Medical Genetics 121A:65–68 (2003)

Clinical Report

Gorlin Syndrome With Ulcerative Colitis in a Japanese Girl

Katsunori Fujii,[1]* Toshiyuki Miyashita,[2] Taku Omata,[1] Kazuhiko Kobayashi,[1] Jun-ichi Takanashi,[1] Katsunori Kouchi,[3] Masao Yamada,[2] and Yoichi Kohno[1]

[1]*Department of Pediatrics, Graduate School of Medicine, Chiba University, Chiba, Japan*
[2]*Department of Genetics, National Research Institute for Child Health and Development, Tokyo, Japan*
[3]*Department of Pediatric Surgery, Graduate School of Medicine, Chiba University, Chiba, Japan*

We present the case of a 14-year-old Japanese girl who had both Gorlin syndrome and ulcerative colitis. She had complained of blood stools for 6 months and severe scoliosis from her infancy. Physical examination revealed multiple nevi, palmar and plantar pits, jaw cysts, and calcification of the falx cerebri, leading to the diagnosis of Gorlin syndrome. Total colonoscopy revealed an edematous and spotty bleeding mucosa extending from the anus to the transverse colon. Histological examination was also compatible with ulcerative colitis. Thus, we diagnosed her as having Gorlin syndrome with ulcerative colitis. Gene analysis revealed a mutation, 1247InsT, in the human patched gene (*PTCH*), resulting in the truncation of PTCH protein. Since Gorlin syndrome and ulcerative colitis are rare disorders in childhood, this association is interesting, suggesting a correlation between the hedgehog signaling and intestinal disorders. © 2003 Wiley-Liss, Inc.

KEY WORDS: Gorlin syndrome; nevoid basal cell carcinoma syndrome; ulcerative colitis; human patched gene; *PTCH*

INTRODUCTION

Gorlin syndrome, also called nevoid basal cell carcinoma syndrome (MIM 109400) [Gorlin and Goltz, 1960], is an autosomal dominant neurocutaneous disease characterized by multiple nevi, basal cell carcinomas, jaw cysts, palmar and plantar pits, calcification of the falx cerebri, and skeletal anomalies [Gorlin, 1987]. The gene responsible for Gorlin syndrome is the human patched gene (*PTCH*) that encodes the receptor for sonic hedgehog protein (SHH) [Hahn et al., 1996; Johnson et al., 1996]. The pathway mediated by SHH is related to the human body conformation, and its disorder causes tumorigenesis and multiple anomalies, such as basal cell carcinomas, holoprosencephaly [Belloni et al., 1996], and developmental defects as seen in Gorlin syndrome.

Here we present an interesting case of Gorlin syndrome associated with ulcerative colitis.

CLINICAL REPORT

The patient, a 14-year-old girl, was in excellent health until 6 months earlier, when she began to experience nausea and watery diarrhea occasionally with fresh blood. Since past 1 month, she had complained of recurrent bloody stools five to six times a week, and was admitted to our hospital for investigation. From her infancy, she had severe scoliosis that was followed up by the Department of Orthopedics in our hospital with surgical intervention. There was no family history of neurocutaneous diseases or congenital malformations. Generally, she was alert but seemed to have mild mental retardation.

Her face was asymmetric, and she had macrocephaly with bossing forehead and hypertelorism. Her trunk was tortuous due to severe scoliosis, and several palmar and plantar pits (Fig. 1A) were recognized. Multiple basal cell nevi were also observed upon her face, trunk, and limbs. Since she never had any sign of malignancy, skin biopsy had not been performed. Abdominal examination revealed mild and diffuse tenderness without defense, although no organ or mass was palpable. Blood examinations showed no specific abnormality except for mild anemia. Radiography of the head and chest revealed calcification of the falx cerebri (Fig. 1B), jaw

*Correspondence to: Katsunori Fujii, Department of Pediatrics, Graduate School of Medicine, Chiba University, 1-8-1 Inohana, Chuo-ku, Chiba-shi, Chiba 260-8677, Japan.
E-mail: kfujii@faculty.chiba-u.jp

Received 12 September 2002; Accepted 22 January 2003
DOI 10.1002/ajmg.a.20082

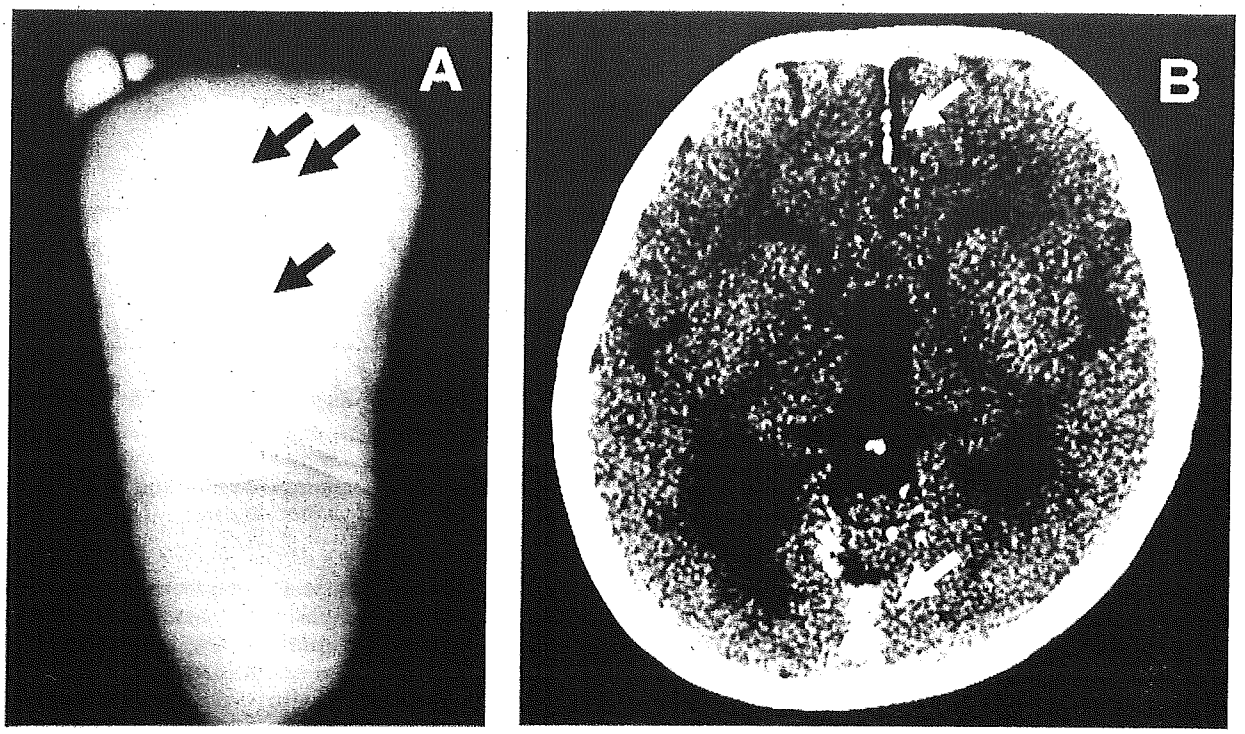

Fig. 1. **A**: Plantar pits (arrow). **B**: Brain CT revealing calcification of the falx cerebri (arrow).

cysts, and the anterior splayed ribs. Stool specimens obtained for culture revealed the normal flora. Endoscopy of the colon revealed diffuse abnormalities, i.e., edema, patchy bleeding, and a loss of the normal vascular pattern continuously extending from the anus to the transverse colon (Fig. 2A). Histological examination of the affected colon showed severe infiltration of inflammatory cells into the mucosa, crypt abscesses, and a decrease in goblet cells (Fig. 2B). No malignant cells were observed in a biopsied specimen. Thus, we diagnosed her as having Gorlin syndrome with ulcerative colitis. The patient was given an intravenous transfusion and salazosulfapyridine. She was also treated with low-diet meals, thereafter the bloody stools gradually disappeared.

After getting written informed consent, we performed *PTCH* gene analysis by direct sequencing of PCR product amplified with primers designed to cover the entire exons as described previously [Fujii et al., 1999]. A heterozygous frameshift mutation, 1247InsT, was identified in exon 9, predicting the truncation of the PTCH protein (Fig. 3). Although we did not analyze her parents' DNA, we assumed that it was a de novo mutation because her parents had presented no symptoms of Gorlin syndrome.

DISCUSSION

The prevalence of Gorlin syndrome has been estimated to be 1 per 57,000 newborns in the United States, and 0.5% of basal cell carcinomas are attributable to this syndrome. The gene responsible for Gorlin syndrome is *PTCH*, the human homolog of the *Drosophila* segmental polarity gene, *patched*. PTCH is a twelve-transmembrane protein and functions as a receptor for SHH, a secreted molecule implicated in the formation of embryonic structures and tumorigenesis. In the girl described here, we identified a novel *PTCH* mutation, 1247InsT, which results in the truncation of PTCH. This is consistent with the previous report that most mutations in Gorlin syndrome lead to a premature termination of the PTCH protein [Wicking et al., 1997].

Current models suggest that the SHH binds to PTCH followed by the induction of the downstream signaling from smoothened (SMO), which is attached to the PTCH protein [Bale and Yu, 2001]. According to this model, the inhibition of SMO signaling is relieved following the truncation of PTCH protein (such as the one identified in our study, resulting in the enhanced downstream signaling from SMO). The signaling can cause developmental anomalies and tumorigenesis in Gorlin syndrome. Although Gorlin syndrome is also called nevoid basal cell carcinoma syndrome, our patient did not develop basal cell carcinoma at the time of diagnosis. This is not unusual, since only half of the patients with Gorlin syndrome develop basal cell carcinoma under age of 20 years [Kimonis et al., 1997]. In this regard, early detection of PTCH mutations may facilitate the detection of basal cell carcinoma or medulloblastoma at an early stage.

Ulcerative colitis is an idiopathic chronic inflammatory bowel disease localized to the colon, sparing the upper gastrointestinal tract. The incidence of ulcerative colitis in school-age children in Europe has been steady at 1.5–2.0 per 100,000 children per year [Ferguson, 1997]. Genome-wide scanning studies have shown a

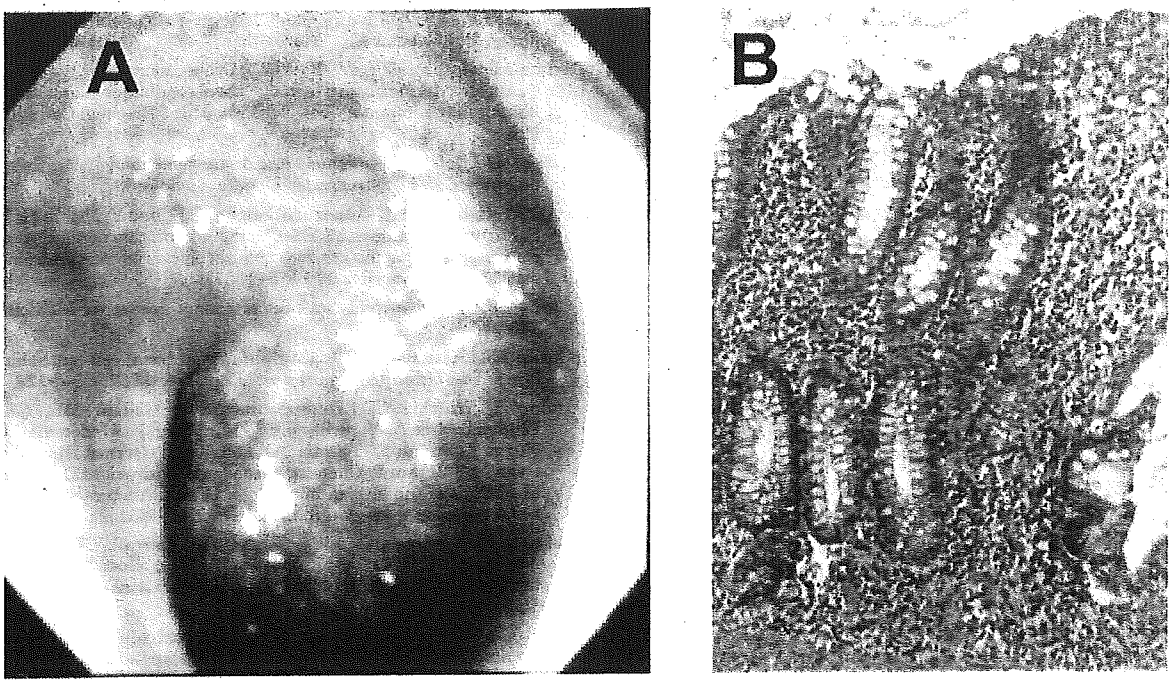

Fig. 2. **A**: Endoscopy of the colon showing diffuse edema, patchy bleeding and a loss of the normal vascular pattern, continuously extending from the anus to the transverse colon. **B**: Histological examination of biopsied affected colon showing moderate to severe infiltration of inflammatory cells into the mucosa, crypt abscesses, and a decrease of goblet cells.

linkage between ulcerative colitis and regions of chromosomes 3, 7, and 12 [Satsangi et al., 1996], although these regions are not related to the Gorlin syndrome locus at 9q22.3. It is also reported that a polymorphism of the mucine gene, *MUC3*, might determine the genetic predisposition to ulcerative colitis [Kyo et al., 1999]. However, many data have suggested that ulcerative colitis also results from environmental factors triggering a breakdown in the regulatory constraints on mucosal immune responses in genetically susceptible individuals. Therefore, its etiology remains to be elucidated.

To our knowledge, there have been two reports of Gorlin syndrome associated with inflammatory bowel

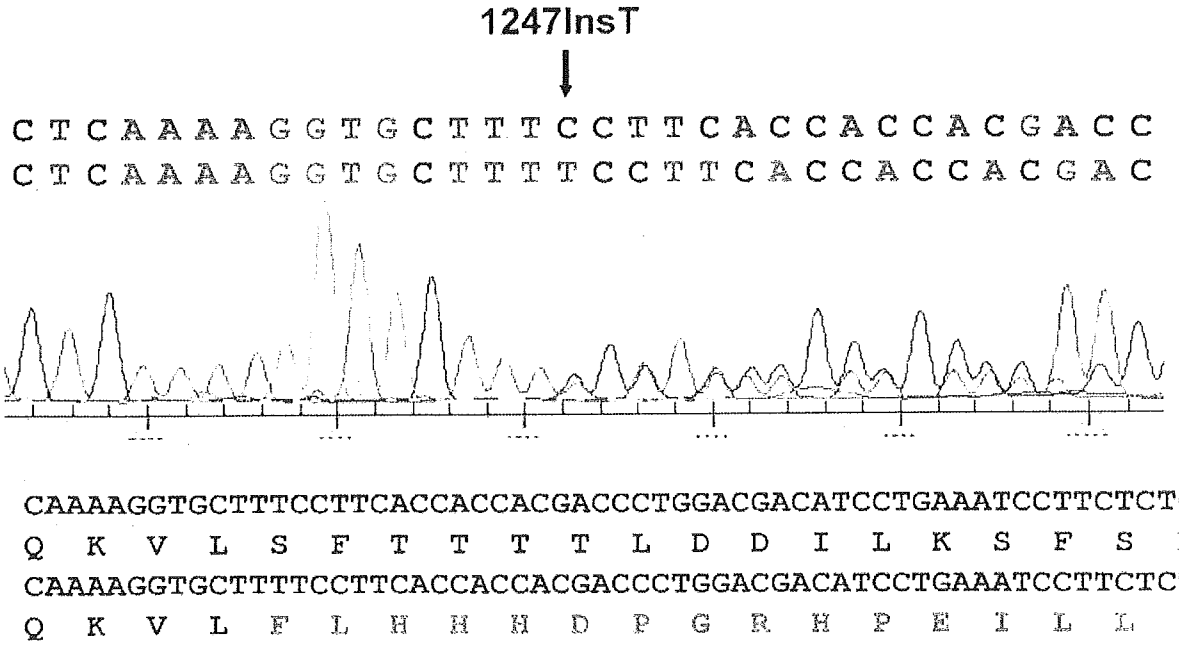

Fig. 3. *PTCH* mutation, 1247InsT, identified in the patient. *PTCH* exon 9 was amplified by PCR and the amplified product was subjected to direct sequencing. The insertion of a thymidine residue is indicated by an arrow. Expected truncation of the PTCH protein is also shown at the bottom. Stop codon is indicated by asterisk.

diseases [Katz et al., 1968; Sawyer and Braverman, 1969]. As they did not show a *PTCH* abnormality, our case is the first report that identified a *PTCH* mutation in a patient with an inflammatory bowel disease. Some other investigators also reported cases of Gorlin syndrome with gastrointestinal polyposis [Schwartz, 1978]. Since it is well known that both ulcerative colitis and gastrointestinal polyposis are prone to develop cancers, some common mechanisms might exist both in Gorlin syndrome and intestinal disorders.

Recently, it was reported that the expression of TGF-β was increased in affected mucosa derived from patients with ulcerative colitis [Babyatsky et al., 1996; Dammeier et al., 1998]. The TGF-β superfamily is a key regulator that modulates mucosal cell populations critical for inflammatory bowel disease, and these members include original TGF-β, activin, bone morphogenetic protein, and decapentaplegic, all of which are thought to exist downstream of the *PTCH* gene. Thus, it is possible that mutant *PTCH* in Gorlin syndrome triggers an enhanced hedgehog signaling, resulting in the increased expressions of TGF-β superfamily in the bowel mucosa, and causes inflammatory bowel diseases.

It is also reasonable to assume that both diseases happened independently, considering a small number of reported cases with two disorders. However, the fact that both Gorlin syndrome and ulcerative colitis are quite rare in childhood tempts us to speculate that there exist some common mechanisms that connect both disorders with each other. Analysis of SHH signaling in inflammatory bowel diseases may help to understand its pathophysiology.

REFERENCES

Babyatsky MW, Rossiter G, Podolsky DK. 1996. Expression of transforming growth factors alpha and beta in colonic mucosa in inflammatory bowel disease. Gastroenterology 110:975–984.

Bale AE, Yu KP. 2001. The hedgehog pathway and basal cell carcinomas. Hum Mol Genet 10:757–762.

Belloni E, Muenke M, Roessler E, Traverso G, Siegel-Bartelt J, Frumkin A, Mitchell HF, Donis-Keller H, Helms C, Hing AV, Heng HH, Koop B, Martindale D, Rommens JM, Tsui LC, Scherer SW. 1996. Identification of *Sonic hedgehog* as a candidate gene responsible for holoprosencephaly. Nat Genet 14:353–356.

Dammeier J, Brauchle M, Falk W, Grotendorst GR, Werner S. 1998. Connective tissue growth factor: A novel regulator of mucosal repair and fibrosis in inflammatory bowel disease? Int J Biochem Cell Biol 30:909–922.

Ferguson A. 1997. Assessment and management of ulcerative colitis in children. Eur J Gastroenterol Hepatol 9:858–863.

Fujii K, Miyashita T, Takanashi J, Sugita K, Kohno Y, Nishie H, Yasumoto S, Furue M, Yamada M. 1999. Gamma-irradiation deregulates cell cycle control and apoptosis in nevoid basal cell carcinoma syndrome-derived cells. Jpn J Cancer Res 90:1351–1357.

Gorlin RJ. 1987. Nevoid basal-cell carcinoma syndrome. Medicine 66:98–113.

Gorlin RJ, Goltz RW. 1960. Multiple nevoid basal-cell epitheliomas, jaw cysts and bifid rib. A syndrome. N Engl J Med 262:908–912.

Hahn H, Wicking C, Zaphiropoulous PG, Gailani MR, Shanley S, Chidambaram A, Vorechovsky I, Holmberg E, Unden AB, Gillies S, Negus K, Smyth I, Pressman C, Leffell DJ, Gerrard B, Goldstein AM, Dean M, Toftgard R, Chenevix-Trench G, Wainwright B, Bale AE. 1996. Mutations of the human homolog of Drosophila patched in the nevoid basal cell carcinoma syndrome. Cell 85:841–851.

Johnson RL, Rothman AL, Xie J, Goodrich LV, Bare JW, Bonifas JM, Quinn AG, Myers RM, Cox DR, Epstein EH, Jr., Scott MP. 1996. Human homolog of patched, a candidate gene for the basal cell nevus syndrome. Science 272:1668–1671.

Katz J, Savin R, Spiro HM. 1968. The basal cell nevus syndrome and inflammatory disease of the bowel. Am J Med 44:483–488.

Kimonis VE, Goldstein AM, Pastakia B, Yang ML, Kase R, DiGiovanna JJ, Bale AE, Bale SJ. 1997. Clinical manifestations in 105 persons with nevoid basal cell carcinoma syndrome. Am J Med Genet 69:299–308.

Kyo K, Parkes M, Takei Y, Nishimori H, Vyas P, Satsangi J, Simmons J, Nagawa H, Baba S, Jewell D, Muto T, Lathrop GM, Nakamura Y. 1999. Association of ulcerative colitis with rare VNTR alleles of the human intestinal mucin gene, *MUC3*. Hum Mol Genet 8:307–311.

Satsangi J, Parkes M, Louis E, Hashimoto L, Kato N, Welsh K, Terwillinger JD, Lathrop GM, Bell JI, Jewell DP. 1996. Two stage genome-wide search in inflammatory bowel disease provides evidence for susceptibility loci on chromosomes 3, 7, and 12. Nat Genet 14:199–202.

Sawyer CS, Braverman IM. 1969. Basal cell nevus syndrome with inflammatory disease of the bowel. Arch Dermatol 99:131–132.

Schwartz RA. 1978. Basal-cell-nevus syndrome and gastrointestinal polyposis. N Engl J Med 299:49.

Wicking C, Shanley S, Smyth I, Gillies S, Negus K, Graham S, Suthers G, Haites N, Edwards M, Wainwright B, Chenevix-Trench G. 1997. Most germ-line mutations in the nevoid basal cell carcinoma syndrome lead to a premature termination of the PATCHED protein, and no genotype-phenotype correlations are evident. Am J Hum Genet 60: 21–26.

MUTATION IN BRIEF

Mutations in the Human Homologue of *Drosophila patched* in Japanese Nevoid Basal Cell Carcinoma Syndrome Patients

Katsunori Fujii[1], Yoichi Kohno[1], Katsuo Sugita[2], Mihoko Nakamura[3], Yoichi Moroi[4], Kazunori Urabe[4], Masutaka Furue[4], Masao Yamada[5], and Toshiyuki Miyashita[5*]

[1]Department of Pediatrics, Graduate School of Medicine; [2]Faculty of Education, Chiba University, Chiba, Japan; [3]Department of Pediatrics, Faculty of Medicine, Kagoshima University, Kagoshima, Japan; [4]Department of Dermatology, Graduate School of Medical Sciences, Kyushu University, Fukuoka, Japan; [5]Department of Genetics, National Research Institute for Child Health and Development, Tokyo, Japan

*Correspondence to: Dr. T. Miyashita, Department of Genetics, National Research Institute for Child Health and Development, 3-35-31 Taishido, Setagaya-ku, Tokyo 154-8567, Japan; Tel.: +81-3-3416-0181; Fax: +81-3-3414-3208; E-mail: tmiyashita@nch.go.jp

Communicated by Mark H. Paalman

Mutations in the human homologue of *Drosophila patched* (*PTCH*) have been identified in patients with nevoid basal cell carcinoma syndrome (NBCCS; also called Gorlin syndrome) as well as sporadic basal cell carcinomas and medulloblastomas. However, using PCR-SSCP analysis, mutations in *PTCH* have been found in only a fraction (about one third to a half) of NBCCS patients. In this study, we determined the whole genomic organizations of the *PTCH* gene and developed a new set of more accurate primers for the analysis of mutations in *PTCH*. Using these primers, we examined 8 Japanese NBCCS patients for mutations in all *PTCH* exons by direct sequencing of the PCR products. As a result, we identified 5 novel *PTCH* mutations in 6 out of 8 patients including 2 sisters as well as 5 polymorphisms, two of them, 1704G>C and 2928G>C were novel. Four of these mutations, 900delC, 1247insT, 1999delC and 933+5G>T, cause protein truncation due to the insertion or deletion of a single nucleotide or aberrant splicing. The remaining mutation, 1514G>A was a missense alteration (G509D). Interestingly, the amino acid substitution, G509V, has been reported previously in an NBCCS patient, suggesting an important role of this amino acid residue in the function of PTCH protein. The difference in the detection rate of *PTCH* mutations among NBCCS between previous reports and ours is due to the difference either in ethnicity or in the detection methods. © 2003 Wiley-Liss, Inc.

KEY WORDS: Gorlin syndrome; NBCCS; PTCH; frameshift; missense mutation; splice variant

INTRODUCTION

Nevoid basal cell carcinoma syndrome (NBCCS; MIM# 109400), also called Gorlin syndrome, is an autosomal dominant neurocutaneous disorder characterized by developmental abnormalities and tumorigenesis [Gorlin, 1987]. Developmental defects include multiple nevi, palmar and plantar pits, jaw cysts, calcification of the falx cerebri, and skeletal anomalies, leading to the diagnosis of NBCCS [Kimonis et al., 1997]. NBCCS is also well known to predispose individuals to cancers such as basal cell carcinoma, ovarian fibroma, medulloblastoma,

Received 5 November 2002; accepted revised manuscript 24 January 2003.

DOI: 10.1002/humu.9132

rhabdomyosarcoma, and cardiac fibroma.

The gene responsible for this disorder is *PTCH*, a human homologue of the *Drosophila* segment polarity gene *patched* (PTCH; MIM# 601309) [Hahn et al., 1997; Johnson et al., 1997]. *PTCH* has been mapped to 9q22.3-q31, and consists of 23 exons encoding 1447 amino acids. The PTCH protein is a receptor for Sonic hedgehog (Shh) and has twelve transmembrane domains. Shh is a secreted molecule implicated in the formation of embryonic structures and tumorigenesis. Thus, a disorder of this pathway could result in an abnormal body conformation and tumorigenesis as seen in NBCCS patients.

Germline mutations of *PTCH* have been reported in NBCCS patients, including nonsense and missense mutations, insertions or deletions, and splicing mutations, although no clustering of mutations has been pointed out. The most common type of *PTCH* mutation is an insertion or deletion that causes a frameshift and leads to a premature truncation of the PTCH protein. Almost all reports about *PTCH* mutations in NBCCS patients have been performed in Caucasian and African-American individuals. Among Asian populations, there have been only two reports describing *PTCH* mutations [Minami et al., 2000; Fujii et al., 1999]. Herein we report novel mutations and polymorphisms of *PTCH* in Japanese patients with nevoid basal cell carcinoma syndrome.

MATERIALS AND METHODS

Subjects and samples

Patients, all of whom were from Japan, were diagnosed according to the clinical criteria of Kimonis et al. [1997]. All studies were approved by the local ethic committee. Of the eight NBCCS cases analyzed, two involve sisters reported previously and 6 are apparently sporadic.

Mutational analysis

DNA from 8 NBCCS individuals was amplified with primers for all but exon 1b (alternative first exon homologous to murine exon 1). This exon could not be amplified because of the extreme GC-rich sequence. New primers were designed to amplify the regions of the *PTCH* gene not covered previously based on GenBank AL161729 (Table 1). All other primers are described previously [Hahn et al., 1996]. Amplified products were gel-purified using the QIAEX II gel extraction kit (QIAGEN) and cycle sequenced with the CEQ™ DTCS-Quick Start Kit (Beckman Coulter) in both directions. The sequence was analyzed on a Beckman Coulter model CEQ™ 2000 DNA sequencer.

Analysis of aberrant splicing by reverse-transcription (RT)-PCR

An immortalized cell line was established from G7 by infection with Epstein-Barr virus (EBV) obtained from B95-8 cells. Total RNA was extracted from EBV-immortalized lymphoblasts with TRIZOL reagent (Invitrogen). RNA was treated with RNase-free DNase I (TAKARA BIO Inc., Ohtsu, Japan) for 2 hours to digest residual genomic DNA and subjected to RT-PCR using the SuperScript™ One-Step RT-PCR kit (Invitrogen). The forward and reverse primers for exon 6 and 7 were 5'-TGGTCATGGTTACATGGACC-3' and 5'-CTGGATAAGCCATGACATCC-3', respectively. The amplified products were also sequenced as described above.

RESULTS

By comparing two reported cDNA sequences of the human *PTCH* gene, GenBank U43148 and U59464, with the genomic sequence, AL161729, that covers the entire *PTCH* gene, the human *PTCH* genomic structure has been determined as described in Figure 1. Since some of the primers reported previously turned out to be incorrectly assigned, new primers were designed to cover all the coding exons of the *PTCH* gene (Table 1).

Table 1. New primers used for mutation analysis of *PTCH*

Exon	Primer sequences	Fragment sizes (bp)
2	PTC2R ACTCCTCCCTTCTGCTTCGT	294
	PTC2R GCGCTGGCGAATATCTCTAT	
10	PTC10F GTTCGGCTTTTGTTCTGTGC	323
	PTC10R CTAGTGGAAAAGGCTGCAAG	
11	PTC11F TGGCAGAGTCCTAACTAGCT	238
	PTC11R TTAGGAACAGAGGAAGCTG	
12a	PTC12F TCTGCCACGTATCTGCTCAC	240
	PTC12R CACCACAGCCTTCATCACCAGAA	
12b	PTC12bF GCATGTTGGTGACCTCTGAA	243
	PTC12bR TCCTTTATAAGTCCACAGGC	
13	PTC13F TGCAACATGTTTCCCCTCCT	452
	PTC13R GAGCCTTAAGTTGTTGTGGCAGA	
15	PTC15F TCTGATGGACGTCTAAGAGC	331
	PTC15R TGTCAAGCAGCCTCCACCAGG	
17	PTC17F AACTGTGATGCTCTTCTACCCTGG	409
	PTC17R TCTTTCTGCAGCCGGGAAGTTTT	
19	PTC19F TAGGACAGAGCTGAGCATTTACC	242
	PTC19R AAACATGTCTCCTTGCACACG	
20	PTC20F ATTTCTGGCGTTGCCATGCT	308
	PTC20R CTGAAGAACCACCAGCAAGT	
21	PTC21F GCCAGCAGGTAAATGGACAA	329
	PTC21R CTGGTTCTGCAGAGTCACTT	
22	PTC22F AAACCCAAGGAGGGAAGTGT	401
	PTC22R AAGCCGTCACAGTGGTGATG	
	PTC22'F TCTACTGAAGGGCATTCTGG	433
	PTC22'R GAACCTTGTCCTCCTCTTTG	

Exons are numbered according to Lench et al (1997).
Two primer pairs are used to amplify exon 22 due to the relatively large size of the exon.

PTCH mutations were identified in 6 out of 8 NBCCS cases examined in this study (Table 2). Like previous reports, the mutations identified in our study also appear to be distributed throughout the gene. To the best of our knowledge, none of these mutations have been reported previously by other groups [Aszterbaum et al., 1998; Chidambaram et al., 1996; Hahn et al., 1996; Hasenpusch-Theil et al., 1998; Johnson et al., 1996; Lench et al., 1997; Minami et al., 2001; Unden et al., 1996; Wicking et al., 1997a,b]. However, a tract of four consecutive deoxycytosines in exon 13, spanning codons 669 to 671 (GAC CCC CAC) seems susceptible to frameshift mutations, since both G3 and a previously reported patient have similar mutations in this stretch (1999delC and 2000insC) [Hahn et al., 1996]. Four out of 6 mutations cause frameshifts resulting in the truncation of the PTCH protein. One of the remaining two patients, G8, carried a missense mutation, G509D. The other, G9, had no mutation within the coding sequence. However, an alteration of the sequence was found in intron 6 (933+5G>T). Despite extensive analysis using RsaI endonuclease, this alteration was not detected in any of 116 unrelated chromosomes (Fig. 2A and data not shown). This point mutation alters the consensus 5' splice site. In order to identify the functional effects of this mutation, we analyzed splicing events between exon 5 and exon 6 by RT-PCR, using the forward primer on exon 5 and the reverse primer on exon 6. The control lymphoblastoid cell line established from a normal individual gave a single RT-PCR product of 150 bp (Fig. 2B, lane 2). Sequencing of this

Table 2. Germ-line mutations and polymorphisms in the *PTCH* gene

Patient	Exon	Mutation[a]	Effect on Coding[b]	Patient's Phenotype
			Missense	
G8	11	1514G>A	G509D	Calcification of falx, multiple BCC, palmar and plantar pits, jaw cysts
			Insertions, Deletions	
G1[c]	6	900delC	Frameshift, truncation	Calcification of falx, multiple nevi, palmar and plantar pits, jaw cysts, macrocephly
G2[c]	6	900delC	Frameshift, truncation	Calcification of falx, multiple nevi, palmar and plantar pits, jaw cysts, macrocephly
G4	9	1247insT	Frameshift, truncation	Calcification of falx, palmar and plantar pits, jaw cysts, hypertelorism, scoliosis, splayed ribs, frontal bossing, mild mental retardation, macrocephly
G3	13	1999delC	Frameshift, truncation	Calcification of falx, multiple BCC, palmar pits, jaw cysts, hypertelorism, short metacarpal
			Splicing	
G9	Intron 6	933+5G>T	Splice variant, truncation	mild mental retardation, palmar and plantar pits, hypertelorism, macrocephly, bifid ribs
			Polymorphisms[d]	
			Tested alleles	**Detected minor alleles**	**Minor allele frequency**	**Reference SNP cluster ID**
	12a	1674C>T	A562A	106	3 heterozygous 1 homozygous	4.7%	rs2066836, rs2227972
	12a	1704G>C	A572A	106	1 heterozygous	0.9%	
	17	2928G>C	G980G	110	12 heterozygous	10.9%	
	21	3571A>T	T1195S	102	6 heterozygous 2 homozygous	9.8%	rs2236405
	22	3932C>T	P1315L	114	28 heterozygous 10 homozygous	42.1%	rs357564

[a] As per Genbank entry U43148, [b] As per Genbank entry U59464, [c] G1 and G2 are sisters and previously reported by Fujii et al., [d] Reference SNP cluster IDs are provided when available

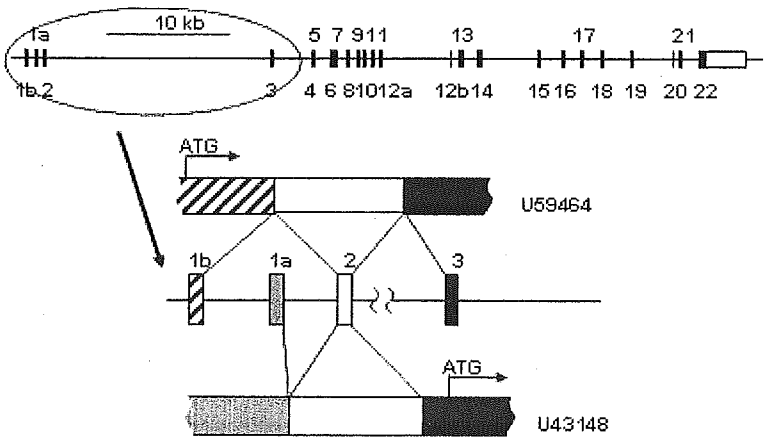

Figure 1. Genomic organization of *PTCH*. The *PTCH* locus based on the sequence AL161729 is shown at the top. Two cDNA sequences, GenBank U43148 and U59464, are generated by alternative splicing using exon 1a and 1b, respectively, as schematically depicted at the bottom. Exon 12b reported firstly by Lench et al (1997) is separated from exon 12a by 6 kb of intronic sequence.

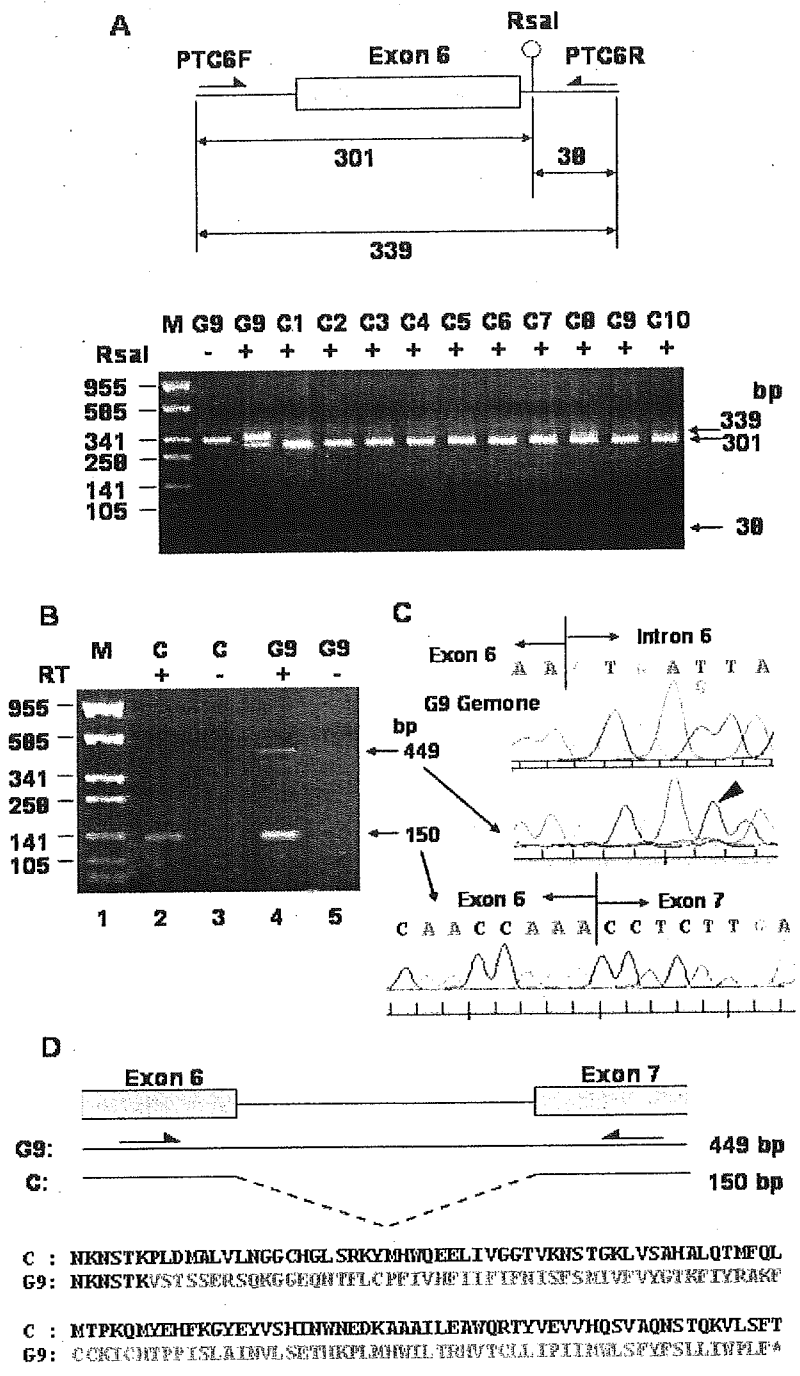

Figure 2. Analysis of the mutation found in G9. **A:** Restriction enzyme analysis of the PCR products. The G to T transition disrupts the RsaI recognition site allowing us to discriminate the mutant allele from the normal one when PCR products are digested with the enzyme. Digested DNA was subjected to electrophoresis on an agarose gel and stained with ethidium bromide. **B:** Analysis of the splicing between exon 6 and 7. RT-PCR was performed using total RNA extracted from lymphoblastoid cells from normal control (C) and G9 in the presence (+) or absence (-) of reverse transcriptase. Primers were designed as described in D. The amplified products were subjected to electrophoresis on an agarose gel and stained with ethidium bromide. **C:** DNA sequence of the PCR products. DNA was extracted from the longer band (middle panel) and the shorter one (lower panel) derived from G9 and directly sequenced with the forward primer used for RT-PCR. Genomic DNA from G9 was similarly sequenced and appears in the top panel. The absence of heterozygosity (G/T) is indicated by an arrowhead. **D:** Abnormal protein translated from a mutant allele. Abnormal amino acids indicated in red are translated due to the absence of slicing between exon 6 and 7 followed by the translational termination (asterisk).

product revealed that this is an authentic splicing product occurring between exon 5 and 6 (Fig. 2C). In contrast, a lymphoblastoid cell line established from G9 gave two distinct RT-PCR products, the expected 150 bp product described above, and the other 449 bp (Fig. 2B, lane 4). Sequencing of the latter product identified a failure of splicing between exon 5 and 6 because the entire sequence of intron 5 was present (Fig. 2C). Contamination by a

small amount of genomic DNA was ruled out since we did not observe any amplified products in the absence of reverse transcriptase in the reaction mixture (Fig. 1B, lane 5). In addition, the larger amplified product contained only the mutated sequence, *i.e.* 933+5G>T, whereas genomic DNA of G9 showed heterozygosity at this site (Fig. 2C, arrowhead). This implies that the larger product was specifically derived from the mutated allele. Translation of this aberrant RNA is expected to produce 107 amino acid residues that are not present in the normal PTCH protein followed by the premature termination (Fig. 2D). Therefore, we conclude that this mutation, like the ones found in G1 to G4, causes protein truncation.

Since 3571A>T/T1195S was initially found in G7, we addressed the question of whether this amino aid substitution exerts any effect on the clinical phenotype seen in G7. By HphI endonuclease digestion of PCR-amplified products, we found 3571A>T/T1195S in 10 out of 102 (9.8%) alleles from unrelated normal Japanese individuals (Fig. 3 and Table 2). In addition, chromosomes homozygous for S1195 were discovered (for example, Fig. 3, lane 7). Altogether, we conclude that this amino aid substitution is unlikely to play a role in the Gorlin phenotype.

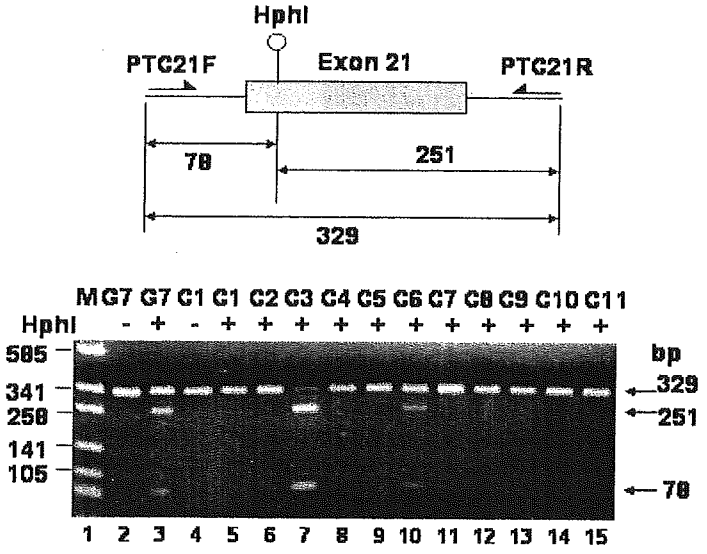

Figure 3. Analysis of the amino acid substitution found in G7. The A to T transition creates a new HphI recognition site allowing us to discriminate both alleles when PCR products are digested with the enzyme. Digested DNA was subjected to electrophoresis on an agarose gel and stained with ethidium bromide.

DISCUSSION

In this study, we identified *PTCH* mutations in 6 out of 8 Japanese patients with NBCCS. As far as we know, only a single study reporting two mutations has been performed in Asian population except for our report on G1 and G2 [Minami et al., 2001; Fujii et al., 1999]. Previously mutations in the *PTCH* gene have been found in 19-32% of NBCCS patients [Chidambaram et al., 1996; Wicking et al., 1997]. Our detection rate for *PTCH* mutations seems higher than previously reported. This may be due to the difference in methodology. In most of the previous reports, patients were initially screened by single strand conformation polymorphism (SSCP), and only samples showing SSCP variants were sequenced. However, several factors such as temperature, pH, running time, gel composition and size of the DNA fragments can influence the sensitivity [Salazar et al., 2002; Jordanova et al., 1997]. Therefore, we performed direct sequencing of the PCR products for entire exons except exon 1b without prior screening by SSCP. It is also possible that the difference in ethnicity influenced the importance of the *PTCH* mutation in the pathogenesis of NBCCS, since previous reports were on Caucasian and African-American patients.

Despite the exhaustive analysis, two patients, G6 and G7, did not show *PTCH* mutations. Failure to detect mutations is likely to be due to the large deletions or existence of mutations in exon 1b or outside the regions analyzed, in introns or regulatory elements. More recently, activating mutations in *Smoothened* and a truncating and a splicing mutation in *PTCH2* have been found in sporadic basal cell carcinomas and medulloblastomas, both of which patients with NBCCS are prone to develop [Xie et al., 1998; Reifenberger et al., 1998; Smyth et al 1999]. Therefore, although families who show linkage to chromosomal regions other than 9q22.3-q31 have not been reported, some of the sporadic NBCCS patients may have mutations in these genes or other genes related to Shh signaling. These possibilities are now under investigation.

Of the six mutations identified, four resulted in truncation of the PTCH protein due to the frameshifts or failure in splicing out the intronic sequence. This is consistent with the report that most (86%) mutations lead to a premature termination of the protein [Wicking et al., 1997]. The significance of the amino acid substitution G509D in patient G8 will not become completely clear until a functional analysis of this mutation is performed. However, we are confident that this is a causative mutation due to the following pieces of evidence. First, the substitution of the same amino acid residue, G509V, has been reported in a Caucasian NBCCS family [Chidambaram et al., 1996]. Moreover, recently, this mutant, G509V, has been proven to be defective in regulating the hedgehog pathway [Taipale et al., 2002]. Second, this alteration was not present in 108 unrelated normal Japanese chromosomes (data not shown) as well as 84 African-American chromosomes [Chidambaram et al., 1996]. Therefore this is unlikely to be a rare polymorphism. Third, PTCH protein has recently been reported to contain sterol-sensing domain (SSD), a motif found in proteins implicated in the intracellular trafficking of cholesterol. Missense mutations in the SSD of *patched*, a *Drosophila* ortholog of the *PTCH* gene, cause an abnormal phenotype of the wing [Strutt et al., 2001; Martín et al., 2001]. G509 is located in SSD and perfectly conserved from *C. elegans* to humans including *Drosophila*. A detailed mutation-function analysis based on the missense mutations found in NBCCS patients would help elucidate the molecular mechanism of the Shh signaling pathway in which PTCH protein is believed to play a key role.

ACKNOWLEDGMENTS

We thank Yuko Ohtsuka, Mami U and Mayu Yamazaki for technical assistance and Kayoko Saito for preparing the manuscript. This study was supported by grants for Brain Research and for Genome Research from the ministry of Health, Labor and Welfare, a Grant-in-Aid for Scientific Research, and a Grant for Organized Research Combination System from the Ministry of Education, Culture, Sports, Science and Technology.

REFERENCES

Aszterbaum M, Rothman,A, Johnson,RL, Fisher,M, Xie,J, Bonifas,JM, Zhang,X, Scott,MP, Epstein,EH, Jr. 1998. Identification of mutations in the human PATCHED gene in sporadic basal cell carcinomas and in patients with the basal cell nevus syndrome. J Invest Dermatol 110: 885-888.

Chidambaram A, Goldstein, AM, Gailani, MR, Gerrard, B, Bale, SJ, DiGiovanna, JJ, Bale, AE, Dean, M. 1996. Mutations in the human homologue of the Drosophila patched gene in Caucasian and African-American nevoid basal cell carcinoma syndrome patients. Cancer Res 56: 4599-4601.

Fujii K, Miyashita,T, Takanashi,K, Sugita,Y, Kohno,H, Nishie,S, Yasumoto,S, Furue,M, Yamada,M. 1999. γ-Irradiation deregulates cell cycle control and apoptosis in nevoid basal cell carcinoma syndrome-derived cells. Jpn J Cancer Res 90: 1351-1357.

Gorlin RJ. 1987. Nevoid basal cell carcinoma syndrome. Medicine 66:99-109.

Hahn H, Wicking, C, Zaphiropoulous, PG, Gailani, MR, Shanley, S, Chidambaram, A, Vorechovsky, I, Holmberg, E, Unden, AB, Gillies, S, Negus, K, Smyth, I, Pressman, C, Leffell, DJ, Gerrard, B, Goldstein, AM, Dean, M, Toftgard, R, Chenevix-Trench, G, Wainwright, B, Bale, AE. 1996. Mutations of the human homolog of Drosophila patched in the nevoid basal cell carcinoma syndrome. Cell 85: 841-851.

Hasenpusch-Theil K, Bataille,V, Laehdetie,J, Obermayr,F, Sampson,JR, Frischauf,AM. 1998. Gorlin syndrome: identification of 4 novel germ-line mutations of the human patched (PTCH) gene. Hum Mutat 11: 480.

Johnson RL, Rothman,AL, Xie,J, Goodrich,LV, Bare,JW, Bonifas,JM, Quinn,AG, Myers,RM, Cox,DR, Epstein,EH, Jr., Scott,MP. 1996. Human homolog of patched, a candidate gene for the basal cell nevus syndrome. Science 272: 1668-1671.

Jordanova A, Kalaydjieva L, Savov A, Claustres M, Schwarz M, Estivill X, Angelicheva D, Haworth A, Casals T, Kremensky I. 1997. SSCP analysis: a blind sensitivity trial. Hum Mutat 10: 65-70.

Kimonis VE, Goldstein, AM, Pastakia, B, Yang, ML, Kase, R, DiGiovanna, JJ, Bale, AE, Bale, SJ. 1997. Clinical manifestations in 105 persons with nevoid basal cell carcinoma syndrome. Am J Med Genet 69: 299-308.

Lench NJ, Telford,EA, High,AS, Markham,AF, Wicking,C, Wainwright,BJ. 1997. Characterisation of human patched germ line mutations in naevoid basal cell carcinoma syndrome. Hum Genet 100: 497-502.

Martin V, Carrillo, G, Torroja, C, Guerrero, I. 2001. The sterol-sensing domain of Patched protein seems to control Smoothened activity through Patched vesicular trafficking. Curr Biol 11: 601-607.

Minami M, Urano, Y, Ishigami, T, Tsuda, H, Kusaka, J, Arase, S. 2001. Germline mutations of the PTCH gene in Japanese patients with nevoid basal cell carcinoma syndrome. J Dermatol Sci 27: 21-26.

Reifenberger J, Wolter, M, Weber, RG, Megahed, M, Ruzicka, T, Lichter, P, Reifenberger, G. 1998. Missense mutations in SMOH in sporadic basal cell carcinomas of the skin and primitive neuroectodermal tumors of the central nervous system. Cancer Res 58: 1798-1803.

Salazar LA, Hirata MH, Hirata RD. 2002. Increasing the sensitivity of single-strand conformation polymorphism analysis of the LDLR gene mutations in brazilian patients with familial hypercholesterolemia. Clin Chem Lab Med 40: 441-445.

Smyth I, Narang, MA, Evans, T, Heimann, C, Nakamura, Y, Chenevix-Trench, G, Pietsch, T, Wicking, C, Wainwright, BJ. 1999. Isolation and characterization of human patched 2 (PTCH2), a putative tumour suppressor gene inbasal cell carcinoma and medulloblastoma on chromosome 1p32. Hum Mol Genet 8: 291-297.

Strutt H, Thomas, C, Nakano, Y, Stark, D, Neave, B, Taylor, AM, Ingham, PW. 2001. Mutations in the sterol-sensing domain of Patched suggest a role for vesicular trafficking in Smoothened regulation. Curr Biol 11: 608-613.

Taipale J, Cooper,MK, Maiti,T, Beachy,PA. 2002. Patched acts catalytically to suppress the activity of Smoothened. Nature 418: 892-896.

Unden AB, Holmberg,E, Lundh-Rozell,B, Stahle-Backdahl,M, Zaphiropoulos,PG, Toftgard,R, Vorechovsky,I. 1996. Mutations in the human homologue of Drosophila patched (PTCH) in basal cell carcinomas and the Gorlin syndrome: different in vivo mechanisms of PTCH inactivation. Cancer Res 56: 4562-4565.

Wicking C, Gillies, S, Smyth, I, Shanley, S, Fowles, L, Ratcliffe, J, Wainwright, B, Chenevix-Trench, G. 1997a. De novo mutations of the Patched gene in nevoid basal cell carcinoma syndrome help to define the clinical phenotype. Am J Med Genet 73: 304-307.

Wicking C, Shanley, S, Smyth, I, Gillies, S, Negus, K, Graham, S, Suthers, G, Haites, N, Edwards, M, Wainwright, B, Chenevix-Trench, G. 1997b. Most germ-line mutations in the nevoid basal cell carcinoma syndrome lead to a premature termination of the PATCHED protein, and no genotype-phenotype correlations are evident. Am J Hum Genet 60: 21-26.

Xie J, Murone, M, Luoh, SM, Ryan, A, Gu, Q, Zhang, C, Bonifas, JM, Lam, CW, Hynes, M, Goddard, A, Rosenthal, A, Epstein, EHJ, de Sauvage, FJ. 1998. Activating *Smoothened* mutations in sporadic basal-cell carcinoma. Nature 391: 90-92.

Zaphiropoulos PG, Unden, AB, Rahnama, F, Hollingsworth, RE, Toftgard, R. 1999. PTCH2, a novel human patched gene, undergoing alternative splicing and up-regulated in basal cell carcinomas. Cancer Res 59: 787-792.

Caspase-8 and caspase-10 activate NF-κB through RIP, NIK and IKKα kinases

Yoshiaki Shikama, Masao Yamada and Toshiyuki Miyashita

Department of Genetics, National Research Institute for Child Health and Development, Tokyo, Japan

NF-κB regulates the expression of various genes involved in cell growth and differentiation, immune response and inhibition of apoptosis. Recently, some death effector domain (DED)-containing proteins, such as FADD and c-FLIP were reported to activate NF-κB. We previously reported that the prodomain-only isoforms of caspase-8 and -10 (PDCasp8/10), containing two DED motifs, could inhibit Fas-mediated apoptosis. Here, we demonstrate that these isoforms also activate NF-κB, implying this to be one of the mechanisms by which these polypeptides inhibit apoptosis. The GST pull-down assay revealed that, among upstream kinases that activate NF-κB, only NIK and RIP, but not RICK or IKKα/β, could directly bind to PDCasp8/10. In addition, both modules of DED in PDCasp8/10 were required for these interactions as well as NF-κB activation. Experiments using a kinase-dead mutant of IKKα and an RIP mutant lacking a kinase domain, both of which function as dominant-negative mutants for their wild-type counterparts, blocked PDCasp8/10-mediated NF-κB activation. Using small interfering RNA technology, we further demonstrate that the down-regulation of IKKα but not IKKβ significantly inhibits PDCasp8-mediated NF-κB activation. Taken together, these results suggest that caspase-8 and -10 have roles in a non- or anti-apoptotic signaling pathway leading to NF-κB activation through RIP, NIK and IKKα.

Received	7/3/03
Accepted	12/5/03

Key words: Apoptosis / Caspases / NF-κB / Death effector domain

1 Introduction

Fas (CD95) and tumor necrosis factor receptor 1 (TNFR1) are the best characterized members of the TNFR family. Upon binding with ligands, these death receptors recruit certain protein molecules to their intracellular death domains, forming death-inducing signaling complex (DISC) [1]. Caspase-8 and -10, two of the apoptosis-inducing cysteine proteases termed caspases, are considered to be recruited in the DISC through binding with the adaptor molecule FADD [2–6]. In the DISC, caspase-8 and -10 are proteolytically activated, and then activate downstream effector caspases. Caspases are synthesized as catalytically dormant proenzymes (procaspases) composed of three domains: large and small subunits of the protease domain, and an N-terminal prodomain [7]. Activated caspases are a hetero-tetramer of two large subunits and two small subunits. The N-terminal prodomains of procaspase-8 and -10 contain two tandemly repeated death effector domain (DED) motifs, which contribute to the interaction with FADD, leading to the DISC formation.

In addition to the apoptosis signal, TNFR1 can induce activation of the anti-apoptotic NF-κB transcription factors [8]. The intracellular portion of TNFR1 interacts with TNFR-associated death domain protein (TRADD) in a TNF-dependent manner, and TRADD acts as an adaptor molecule to recruit various protein molecules such as FADD/MORT1, RIP, and TNFR-associated factor 2 (TRAF2) [9]. RIP is a death domain-containing kinase that is crucial for NF-κB activation, while TRAF2 activates the MAP kinases [10–12]. NF-κB is activated in response to many signals such as IL-1, lipopolysaccharide, as well as TNF-α , and has been shown to regulate a wide variety of genes that are involved in cell growth, differentiation, inflammatory responses, or the regulation of apoptosis [13]. NF-κB transcription factors exist in a latent, inactive form sequestered in the cytoplasm by a family of inhibitors of NF-κB (IκB) proteins. The phosphorylation of IκB by IκB kinase (IKK) complex leads to the degradation of IκBs and the translocation of NF-κB transcription factors into the nucleus. Therefore, the activation of IKK complex is thought to be the convergent point of various signaling pathways that activate NF-κB. IKK complex con-

[DOI 10.1002/eji.200324013]

Abbreviations: DED: Death effector domain **IKK:** IκB kinase **NIK:** NF-κB-inducing kinase **PDCasp8/10:** Prodomain-only isoforms of caspase-8/10 **siRNA:** Small interfering RNA **IκB:** Inhibitor of NF-κB **Mt:** Mutant

0014-2980/03/0707-1998$17.50+.50/0

tains three IKK polypeptides. Two of these polypeptides, IKKα and IKKβ, are catalytic subunits, while the third, IKKγ, is regulatory [14].

Recently, it was reported that DED-containing polypeptides, such as c-FLIP, FADD, and caspase-8 and -10, could induce NF-κB activation [15, 16]. This result indicates that, in addition to apoptosis pathways, caspase-8 and -10 may be involved in anti-apoptosis signaling pathways. Interestingly, both caspase-8 and -10 have isoforms that lack protease domains [2, 17]. In our recent report, we demonstrated that the prodomain-only polypeptides of caspase-8 and -10 (PDcasp8 and PDCasp10), analogous to the isoforms above, specifically inhibited death receptor-induced cell death, and that this ability to inhibit cell death required both of the DED motifs [18]. Here, we provide evidence that PDcasp8 and PDCasp10 can induce NF-κB activation, and again, this ability requires the two DED motifs. Taken together, it is intriguing to speculate that prodomain-only isoforms of caspase-8 and caspase-10 inhibit death receptor-mediated cell death by inducing NF-κB-regulated anti-apoptotic gene expression. We further discuss the mechanism by which these molecules cause the activation of NF-κB transcription factor.

2 Results

2.1 Caspase-8 and caspase-10 selectively activate NF-κB and both modules of the DED domain are required for the activation

Recently, it was reported that caspase-8 and -10 can activate NF-κB transcription factor [15, 16]. Since CARD domain-containing proteins such as Bcl-10 and CARD4 are also reported to activate NF-κB [19, 20], and caspase-2 and caspase-9 have a CARD domain in their N-terminal prodomains, we first investigated the selectivity of caspase-mediated NF-κB activation. Interestingly, among the caspases analyzed, only DED-containing caspases activated NF-κB (Fig. 1A). It is unlikely that the deficient activation by other caspases was due to cell loss, since their cell death-inducing activities are much less potent than those of caspase-8 and -10 when overexpressed [21] and, moreover, carbobenzoxy-VAD-fluoromethyl ketone (zVAD-fmk), a caspase inhibitor with a broad spectrum, was used to prevent cell death after the transfection. Protease-dead mutants of caspase-8 or -10, or PDCasp8 or PDCasp10, were equally potent in activating NF-κB, suggesting that the protease activity is not required and DED-containing prodomains are sufficient for NF-κB activation.

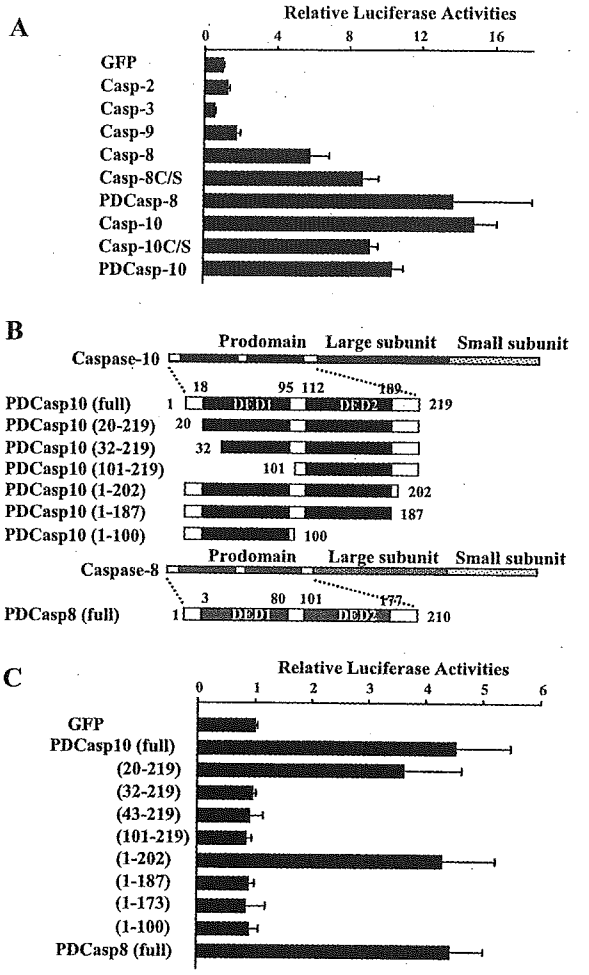

Fig. 1. Activation of NF-κB by caspases and their mutants. (A) 293 cells were transfected with 0.5 μg of indicated expression plasmids for various caspases and their protease-dead mutants (C/S) in combination with 0.5 μg 3X-κB-luciferase and 0.5 μg β-galactosidase plasmid. The cells were harvested at 24 h after transfection, and used for luciferase assays. A plasmid for EGFP non-fusion protein (GFP) was used as a control, because all caspases were expressed as GFP fusions. (B) Expression plasmids encoding various deletion mutants used in (C) are depicted. Numbers refer to amino acid positions. (C) 293 cells were transfected as described in (A), and a luciferase assay was performed.

Both caspase-8 and -10 have a tandem repeat of the two DED domains. To address the question of whether one or both of the DED motifs are required for NF-κB activation, various deletion mutants of PDCasp10 were generated as depicted in Fig. 1B and subjected to an NF-κB reporter assay. When 20 or less amino acid residues were deleted from either N or C terminus of PDCasp10, the mutants retained the ability to induce NF-κB activity. In contrast, mutants with 30 or more amino acid dele-